A Method to Define Low-Altitude Rocket Exhaust Characteristics and Impingement Effects

E. T. PIESIK* AND D. J. ROBERTS*
General Dynamics, Pomona, Calif.

Semiempirical methods are used to describe the free flowfield from a moderately underexpanded nozzle and to predict the normal impingement effects of pressure and heat-transfer to a flat plate. Results compare favorably with data obtained from the literature and from impingement tests using a highly aluminized solid propellant rocket. In the free flowfield, the supersonic core length and the subsonic, centerline, recovery pressure and temperature distributions are determined from empirical equations. Simplifying assumptions are made in the supersonic region which smooth the complex flow and discontinuities that really exist. Radial distributions are based on the conservation of momentum, the assumption of a Gaussian momentum distribution, and the one-dimensional isentropic flow equations. The Fay-Riddell heating equation describes the laminar stagnation region on the plate. Otherwise, the Van Driest turbulent heating equation is used with the velocity gradient dependent on the plate recovery pressure gradients.

Nomenclature

A = area
c_p = specific heat
D = diameter
g = gravitational constant
h = heat-transfer coefficient
i = enthalpy
Le,M = Lewis and Mach numbers, respectively
$\dot{m}$ = mass flow
P = pressure
Pr = Prandtl number
q = dynamic pressure = $\rho u^2/2$
$\dot{q}$ = heat flux; $\dot{q}_c$, convective; $\dot{q}_r$, radiative
R = gas constant
Re = Reynolds number
r = radius or radial flow length
$r_{1/2}$ = radius at the half velocity
T = temperature
u = velocity
X = axial distance from nozzle exit
β = velocity gradient
γ = specific heat ratio
μ = viscosity
ρ = density
Φ = axial moment; Φ_t is defined by Eq. (5)

Subscripts

c = chamber (or convective, with $\dot{q}$)
cc = constant core
cl,cw = centerline and cold wall, respectively
D = dissociation
e,ex = jet edge and exit, respectively
g,i = gas and plate flow, respectively
k = kth ring in plate flow analysis
opt = optimum (after isentropic change from P_{ex} to P_∞)
R,s = recovery and stagnation, respectively
r = plate radius
ss,sup = sonic tip and supersonic, respectively
t,w = total and wall, respectively
$2,\infty$ = downstream of shock, and ambient, respectively

Presented as Paper 69-568 at the AIAA 5th Propulsion Joint Specialist Conference, U.S. Air Force Academy, Colo., June 9–13, 1969; submitted June 11, 1969; revision received January 21, 1970. The study was supported by the FMC Corp., Northern Ordnance Division under Contract P.O.H.-65620 and this paper is based on Ref. 1.

* Design Specialist, Aerothermodynamics, Pomona Division.

Introduction

THIS paper describes semiempirical methods for the prediction of the pressure and heat-transfer effects of the exhaust from a stationary (or slowly moving) rocket impinging normally on a flat surface at sea level (Fig. 1). The problem is divided into three parts: 1) definition of the flow parameters of the free exhaust (which may be anywhere from overexpanded to moderately underexpanded) by use of empirical relations for the centerline variations of the parameters and Gaussian distribution to describe radial distributions; 2) definition of the flow parameters on a flat surface resulting from normal impingement of the free exhaust; and 3) the heat-transfer definition using the plate flow model parameters and the well-known heat-transfer equations of Fay and Riddell, and Van Driest.

Free Exhaust Flowfield

We assume that P_c, T_c, R, γ, D_{ex}, and M_{ex} are known, and that the static pressure in the exhaust flowfield is everywhere equal to the ambient pressure (P_∞ = 14.7 psia). The descriptions of the centerline distributions of recovery pressure and temperature in the subsonic region rely heavily on the data of Refs. 2–12, from which the following empirical equations are derived. The location of the sonic tip on the centerline is given by

$$X_{ss}/D_{opt} = 150\Big/\left\{\left[\frac{1000\{[(1+\gamma)/2]^{\gamma/(\gamma-1)}-1\}}{P_{topt}/P_\infty - 1}\right]^{1/(0.235M_{opt}+2.03)}\right\} \quad (1)$$

and the total recovery pressure ratio for $X \geq X_{ss}$ is given by

$$(P_{t2}-P_\infty)/(P_{topt}-P_\infty) = 0.001(150\,D_{opt}/X)^{0.235M_{opt}+2.03} \quad (2)$$

It is assumed that mixing of ambient air with the exhaust occurs only in the subsonic portion of the exhaust flow. (Some supporting evidence can be derived from the gas probe data of Ref. 13.) Thus, for $X < X_{ss}$, the total temperature will be equal to T_{tc}. For $X \geq X_{ss}$,

$$(T_{cl}-T_\infty)/(T_c-T_\infty) = 0.1[X/(150D_{opt})]^{1/\log_{10}[X_{ss}/(150D_{opt})]} \quad (3)$$

In these equations the subscript "opt" refers to conditions

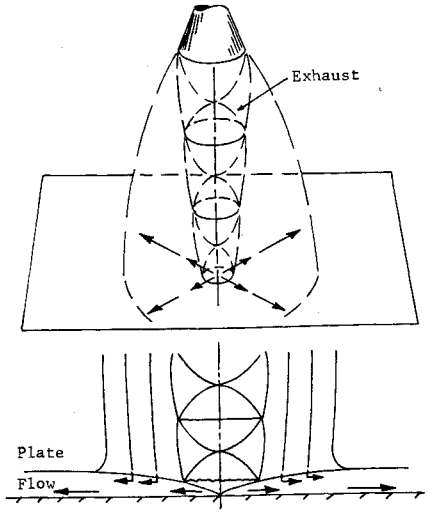

Fig. 1 Typical exhaust and plate flow.

that would exist after isentropic expansion or contraction of the nozzle exit flow from P_{ex} to P_∞. For simplicity we assume that these optimum conditions would be achieved at the nozzle exit ($X_{opt} = X_{ex} \equiv 0$). (The actual location of optimum expansion would be either in the nozzle for an overexpanded flow or within $X/D_e < 2$ for a moderately underexpanded nozzle, but the exact location is difficult to determine.)

The shock structure in the supersonic region dictates that M_{cl}, on average, decreases with distance. Because this region is in fact so complex, the simplifying assumption is made that M_{cl} varies exponentially from 1.0 at the sonic tip ($X = X_{ss}$) to M_{opt}:

$$M_{cl} = M_{opt}e^{-X/X_{ss}\ln M_{opt}} \tag{4}$$

Obviously this M_{cl} distribution is arbitrary, but for $X/D_{ex} > 5$ it describes the available data quite well (Fig. 2). In the first few diameters, normal shocks are occurring for some cases (e.g., Fig. 2, top), but the subsonic flow that exists locally downstream of the normal shocks is accelerated to $M_{cl} > 1$ again due to the peripheral flow conditions of the exhaust. Cold-air data in terms of u_{cl}/u^* are compared in the lower part of Fig. 2. Typical centerline pressure distribution data are compared with the predictions based on Eqs. (2) and (4) in Fig. 3.

Literature data dealing with recovery temperatures of a high-enthalpy supersonic exhaust are scarce, but Fig. 4 compares the results of Eq. (3) with the data of one available survey.[14]

Table 1 presents the characteristics of the various nozzles and rocket engines for the data used in the various comparisons presented herein. A statistical comparison of the predicted [Eq. (1)] and measured values of X_{ss} shown in the last column of Table 1 indicates a standard deviation of 13%.

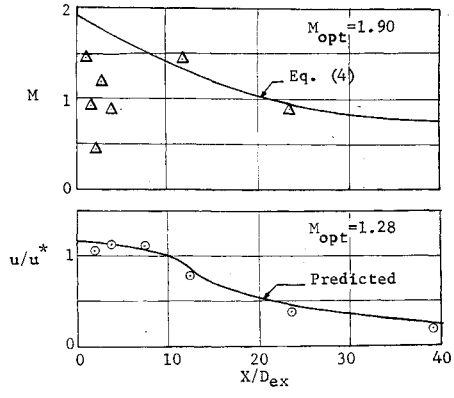

Fig. 2 Centerline velocity distributions-air data.[3]

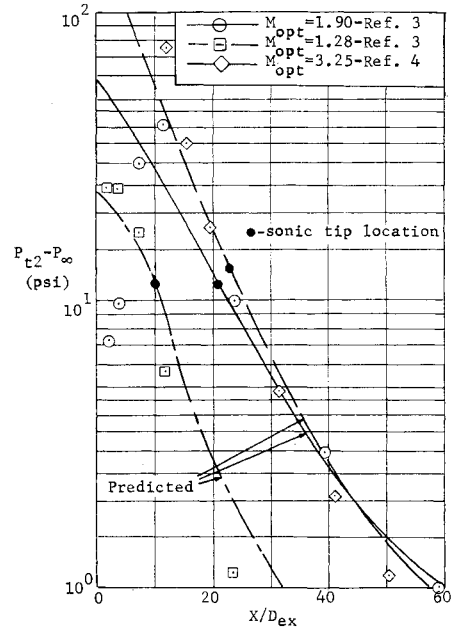

Fig. 3 Centerline recovery pressures.

The primary requirement to be satisfied in the analysis of the radial distribution of the free flowfield is that the total momentum Φ_t which exists at the optimum conditions is conserved; i.e.,

$$\Phi_t = 2\pi \int_0^\infty \rho u^2 r dr \equiv \gamma P_\infty M_{opt}^2 A_{opt} \tag{5}$$

wherein $\rho u^2 = \gamma P M^2 \equiv 2q$. Because the flow in the supersonic region is very complex and some averaging of the flow is needed for the model, it is assumed that there exists in the supersonic region a flow in which gas-dynamic properties are constant within any plane normal to the centerline. The radius of this flow is assumed to be proportional to $(M_{cl} - 1)$:

$$r_{cc} = r_{opt}(M_{cl} - 1)/(M_{opt} - 1) \tag{6}$$

The gasdynamic properties for this flow are the centerline values at each X. The assumption of a constant-property centercore is somewhat substantiated by Ref. 3.

The radial flow parameters are obtained through the assumption that the momentum distribution outside the constant-property core and in the subsonic region takes the shape of a normal curve (gaussian distribution):

$$q = q_{cc}e^{-Kr^2} \tag{7}$$

The total momentum of the jet at some particular axial location can now be considered in two parts: the constant-property core region and the normal distribution region.

$$\Phi_t = \Phi_{cc} + 2\pi \int_{r_{cc}}^\infty 2q_{cc}e^{-Kr^2} r dr \tag{8}$$

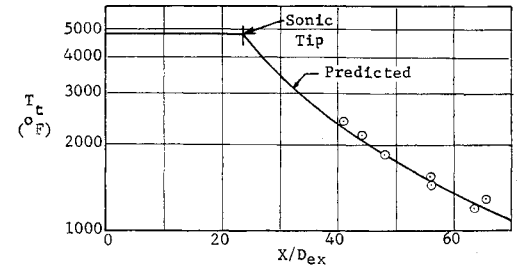

Fig. 4 Centerline recovery temperature.

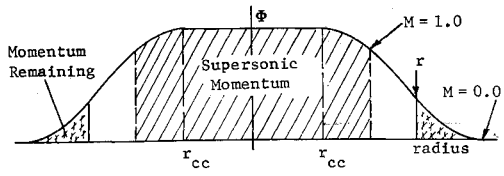

Fig. 5 Mixing region model.

where $\Phi_{cc} = \pi r_{cc}^2 P_\infty \gamma M_{cc}^2$. Integration of Eq. (8) gives

$$\Phi_t = \Phi_{cc} + 2\pi q_{cc} e^{-Kr_{cc}^2}/K \tag{9}$$

The value of K for each axial location ($X < X_{ss}$) is determined by solving $e^{-Kr_{cc}^2}/K = (\Phi_t - \Phi_{cc})/(2\pi q_{cc})$ either graphically or by trial and error. All the terms on the right side of the equation are known as is r_{cc}. For $X \geq X_{ss}$, K is evaluated directly for each axial location since $r_{cc} = 0$ and $q_{cc} = q_{cl} = P_{t2} - P_\infty$; thus

$$K = 2\pi q_{cl}/\Phi_t \tag{10}$$

The relationship between Φ and r can be obtained by integrating

$$\Phi = \Phi_{cc} + 2\pi \int_{r_{cc}}^{r} 2q_{cc} e^{-Kr^2} r dr$$

and manipulating the result:

$$r = \{\ln[e^{-Kr_{cc}^2} - K(\Phi - \Phi_{cc})/(2\pi q_{cc})]^{-1}/K\}^{1/2} \tag{11}$$

In the mixing (subsonic) region, Fig. 5, the radial distribution of the mass fraction of ambient air $\alpha = \alpha(r)$, at a particular station (X) is assumed to be dependent upon the momentum distribution:

$$\alpha(r) = 1 - (\Phi_t - \Phi)/(\Phi_t - \Phi_{sup}) \tag{12}$$

The gas properties (T_t,T,γ) required for the flowfield predictions at any radius in the subsonic region are taken as the bulk averages of the exhaust/air constituents. Figure 6 compares normalized T_t data from Ref. 2 with results derived from Eqs. (3, 11, and 12).

In summary, q and/or M are defined at all axial and radial locations through Eqs. (1, 2, 4, 6, and 7) and the evaluation of K. The recovery temperature is obtained with Eqs. (3, 11, and 12). If use is made of the well known isentropic flow equations and the flow parameters determined up to this point, the free exhaust flowfield is now completely defined for any gaseous sonic or supersonic nozzle flow undergoing a moderate expansion (or contraction) to P_∞.

Flat Plate Flow

The flow parameters parallel to the flat plate after the normal impingement of the exhaust are based upon a simple mixing theory. It is assumed that at any radial location in the free exhaust the flow approaches the plate (negotiating a normal shock where necessary) and instantaneously turns parallel to the plate, completely mixing with any plate flow up to that location (see Fig. 1). It is further assumed that the $P(r)$ on the plate can be closely approximated as being equal to the free exhaust's $P_{t_2}(r)$. Figure 7 compares measured $P_{t_2}(r)$ distributions with the flat plate pressure data and the $P_{t_2}(r)$ predicted by the method in this paper.

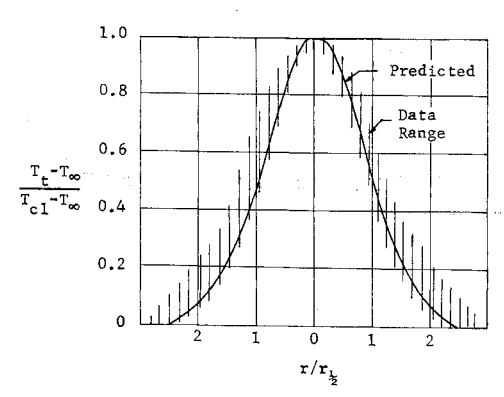

Fig. 6 Radial total temperature distribution.

Table 1 Data synopsis and comparison of predicted and measured values of X_{ss}

Ref.		γ	M_{ex}	P_{ex}/P_∞	D_{ex}, in.	X_{ss}/D_{opt} pred./meas.
1	SP[a]	1.2	3.06	3.78	7.2	41.6
2	SP	1.25	3.53	1.22	2.0	37.9/39.1
		1.28	2.82	1.41	2.59	30.5/25.8
			3.42	0.88	2.56	34.3/36.5
3	Air	1.4	1.0	1.15	0.51	8.4/8.7
				1.42	0.51	10.1/9.5
				2.88	0.51	15.6/16.2
				3.57	0.51	17.3/17/3
				4.36	0.51	18.7/19.8
4	LP[a]	1.24	3.76	0.4	7.0	33.2/31.7
5	Air	1.4	1.5	1	...	12.5/9.5
				2	...	17.8/13.6
				5	...	24.8/23.5
				10	...	30.1/25.3
			3.0	1	...	30.1/30.0
				2	...	35.7/40.0
6	Air	1.4	1.4	1	0.74	11.4/13.5
7	Air	1.4	2.6	1	2.55	25.4/28.0
8	SP	1.24	3.13	1.41	17.75	34.2/31.6
9	SP	1.25	2.69	2.79	5.1	33.4/27.5
10	N_2	1.4	3.3	1.51	...	37.1/33.3
				0.60	...	29.6/37.0
	CH_4	1.31	3.1	1.45	...	34.2/35.1
11	Air	1.4	2.96	1.60	0.38	33.4/36.3
			2.3	4.43	0.25	33.4/30.6
	LP	1.24	3.22	0.52	1.50	28.6/28.4
12	Air	1.4	2.22	1.00	1.01	20.9/25.1

[a] Working fluid: SP = solid propellant, LP = liquid propellant.

Some of the surface-pressure data from Ref. 14 for highly-aluminized-propellant, rocket-exhaust impingement tests,† for axial locations less than half way down the supersonic flow length, are presented in Fig. 8. The figure shows good correlation for $r > r_{cc}$; the poor correlation near the centerline can be at least partially attributed to normal shocks occurring in this region.

The flow parameters on the plate are readily determined from the gas-dynamic relations and the equation of continuity if one allows the impinging normal flow to be divided into concentric rings k ($k = 1, 2, \ldots n$) which are thin enough that the flow parameters can be considered constant within each ring. Starting at the center, the flow across the radial boundary of each ring is calculated. Mach number along the plate surface is determined using the free-exhaust $P_{t_2}(r)$ and the $P_t(r)$ of the flow along the plate. Remember that $P(r)$ on the plate is equal to $P_{t2}(r)$. Thus, $P_t(r)$ along the plate is composed of the partial pressure of the flow on the plate up to that ring plus the partial pressure of the flow coming into the ring from the free exhaust.

The $T_t(r)$ of the plate flow is the bulk average of all flow rings from the jet centerline up to and including the ring k in question. Similarly, $\dot{m}(r)$ is simply the total mass flow for

† The tests consisted of actual missile launchings with a flat plate positioned behind the nozzle and normal to the exhaust axis. Since the missiles were not vertically launched, the point of intersection of the exhaust axis on the plate moved down the plate (due to the gravity component) as the missile moved forward. Thus, the relative position of the instrumentation with respect to the exhaust axis continually changed.[14]

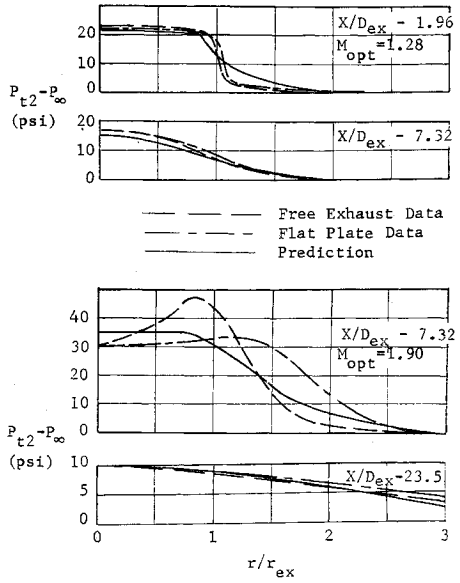

Fig. 7 Recovery pressure comparison.

all rings through ring k. With M_k and T_{tk} defined, T_k and u_k are easily obtained.

Numerous plate gas temperature data were obtained during the tests of Ref. 14. These data are in substantial agreement with predictions. A typical T_{gw} history is presented in Fig. 9.

Heat-Transfer Analysis

For convective heating, the gas impinging on the flat plate can be divided into three regions (Fig. 10) which require slightly different treatments: 1) the exhaust core impingement region, 2) the region of high pressure gradient dP/dr just outside the core, and 3) the essentially constant-pressure region at large distances from the jet axis. In region 1 (which is of concern only when the plate is located at $X < X_{ss}$), the free exhaust flow properties, u, P, and T, are constant at each X. It is assumed that the velocity gradient on the plate ($\beta = du/dr$) is constant in this region, so the heat-transfer coefficient h varies only with distance r from the center. In region 2, the flow is rapidly accelerated, so that β is high and varies rapidly. In region 3, $P_{t_2} \rightarrow P_\infty$, and u is nearly constant but at great distances begins to decline; this is similar to constant velocity flow over a flat plate.

Two equations are used to predict $\dot{q}_c$ for the entire flowfield. For $\dot{q}_{cc_l}$, the laminar stagnation region equation of Fay-Riddell[17] is used. Otherwise, $\dot{q}_c$ is predicted using the Van Driest equation for turbulent stagnation region heating. It is necessary only to modify the β term in each of the three defined flow regions.

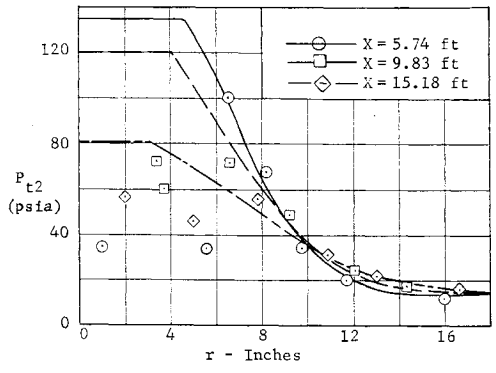

Fig. 8 Radial pressure distribution comparison.

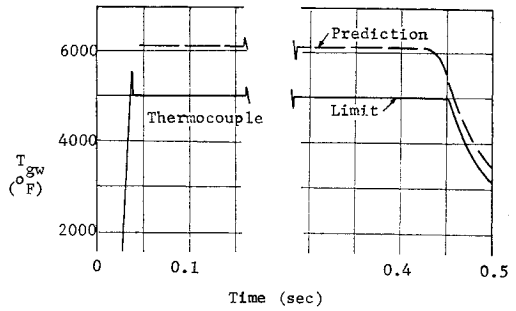

Fig. 9 Typical plate gas temperature comparison.

The basic Fay-Riddell equation for laminar flow heat flux is[17]

$$\dot{q}_c = 0.76(\rho\mu)_w^{0.1}(\rho\mu)_s^{0.4}[1 + (Le^{0.52} - 1) \times (i_D/i_s)]\beta^{1/2}(i_s - i_w)/Pr^{0.6} \quad (13)$$

For air, $Le \simeq 1.4$; for rocket exhausts, Le is not known, but for a mixture containing a light component such as H_2, Le can vary from 0.25 to 3.5, depending on the H_2 concentration.[18] However, considering the degree of dissociation in a typical rocket exhaust, the enthalpy ratio i_D/i_s should not be larger than 0.165. Thus, the maximum possible variation for the bracketed term is 0.92 to 1.13. Therefore, we shall assume that the term in the brackets is unity.

The primary parameter to be determined in Eq. (13) is the velocity gradient β. (For hemispherical stagnation-point heating β can be evaluated based on Newtonian Theory, but this method is not applicable to a flat plate.) An expression for β recommended for fully developed exhaust jet flow[3] has been extended for use in region 1 by reducing the radius of the half velocity $r_{1/2}$ by the radius of the constant-property core of the free exhaust:

$$\beta_s = 1.13u_{cl}/(r_{1/2} - r_{cc}) \quad (14)$$

Using Eqs. (13) and (14), a comparison is made in Fig. 11 of the centerline, cold-wall-total-heat-flux data from Ref. 4 with the sum of predicted $\dot{q}_c$ and measured radiant heat flux $\dot{q}_r$.

For $r > 0$, the general convective heat flux equation is appropriate:

$$\dot{q}_c = hA(i_R - i_W)/c_p \quad (15)$$

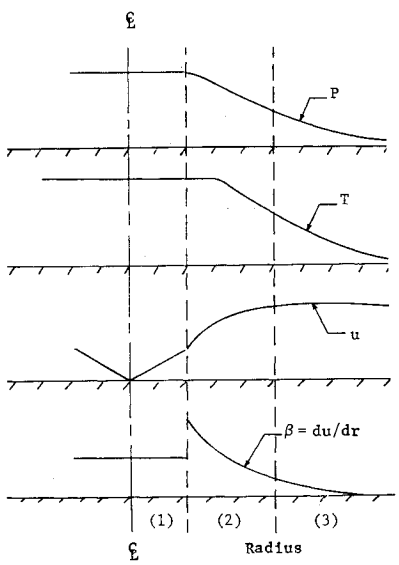

Fig. 10 Flow region for flat plate heat transfer.

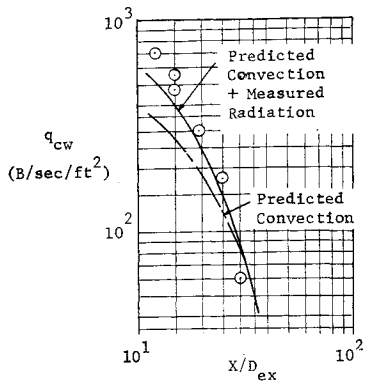

Fig. 11 Centerline heat flux comparison.

For h we use local flow properties and the Van Driest equation[10]:

$$h = 0.042P_r^{-2/3}(\rho^4\mu\beta^4r^3)^{1/5}c_p \quad (16)$$

In the core region, where $u = u_{cl}$ for the free exhaust, β = constant = β_s as given by Eq. (14). In region 2, β is the local velocity gradient: $\beta = \Delta u/\Delta r$. In region 3, when $\Delta u/\Delta r \leq u/r$, we assume that $\beta = u/r$, and Eq. (16) takes the form for flow at constant velocity:

$$h = 0.042P_r^{1/3}R_e^{4/5}k/r \quad (17)$$

To account for compressibility effects, Eq. (16) is modified using Eckert's reference enthalpy method; i.e., Eq. (16) is multiplied by $(i/i^*)^{4/5}(\mu/\mu^*)^{-1/5}$, where the reference enthalpy is calculated from

$$i^* = 0.28i + 0.5i_w + 0.22i_R \quad (18)$$

Heat-Transfer Data Comparison

Up to this point the discussion has been concerned with gas-phase exhausts only. The heat-flux comparisons to be discussed here were obtained from Ref. 1. This rocket exhaust contained approximately 40% Al_2O_3 (as solid or liquid).[19] However, for simplicity we assume that the entire exhaust is in the gas phase. As is shown in Figs. 8 and 9 and Ref. 1, the applicability of the predicted plate impingement parameters of pressure and gas temperature is apparently not strongly affected by this assumption. Although particle impact heating (which is neglected) might be expected to be rather severe initially, a compensating insulating effect would be expected as solid Al_2O_3 built up on the impinged surface.

Total heat flux ($\dot{q}_t$) data from eleven slug calorimeters were compared to predictions during the study of Ref. 1; however, a slug calorimeter does not distinguish between heating due to convection, radiation, or particle impingement, and it was not possible to extract a meaningful cold-wall $\dot{q}_c$ from the data. The comparison was made using the total hot wall heat flux. The predicted hot wall $\dot{q}_c$ was added to a conservative estimate of $\dot{q}_r$, assuming an opaque plume. The shape factor was assumed to be unity. The emissivity of the exhaust was taken conservatively to be 0.7, even though the literature indicates a fairly low particle emissivity (about 0.25) for Al_2O_3 at $T > 3000$°R. The gas temperature was assumed to be that of the local gas flow over the plate. Using this conservative simplified approach, $\dot{q}_r$ has a maximum of 4 Btu/in.^{2}-sec at the center of the jet.

Unfortunately, the heat-transfer data comparison does not allow a definite conclusion concerning the acceptability of the "all gas" assumption for Al_2O_3. Figure 12 compares predicted and measured $\dot{q}_t(t)$ histories for two calorimeter locations.

A $\dot{q}_t$ comparison for the first 0.5 sec of data was obtained by integrating the heat flux curves of Ref. 1. The average difference between the predicted and the measured values was ~23%. The differences varied from 3% to 43% for nine measurements; two calorimeters were not included because they failed prior to 0.5 sec.

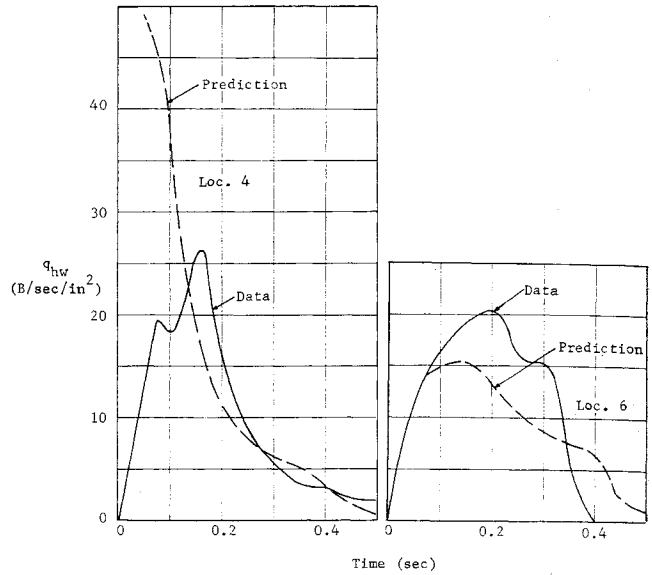

Fig. 12 Aluminized solid-propellant heat flux.

Concluding Remarks

In general, the semiempirical prediction described herein gives results for both the free flowfield parameters in a rocket's exhaust and the effects of its normal impingement on a flat plate that may be useful for preliminary design estimates. However, the method does not adequately predict the supersonic portion of the exhaust near the nozzle exit, if normal shocks are occurring. For two-phase exhausts, the assumption that the Al_2O_3 particles can be treated as gas apparently is acceptable in the determination of flat-plate recovery pressure and gas temperature, but its effect on the modeling of heat-transfer is not known.

References

[1] Piesik, E. T., Roberts, D. J., and Dershin, H., "Final Report: Rocket Exhaust Impingement Study," CR-6-332-762-001, Aug. 1968, General Dynamics, Pomona, Calif.

[2] Anderson, A. R. and Johns, F. R., "Nondimensional Characteristics of Free and Deflected Supersonic Jets Exhausting into Quiescent Air," NADC-ED-5401, March 1954, U.S. Naval Air Development Center, Johnsville, Penn.

[3] Snedeker, R. S. and Donaldson, DuP. C., "Experiments on Free and Impinging Underexpanded Jets from a Convergent Nozzle," Rept. 63, DDC AD 461622, Sept. 1964, Advanced Research Projects Agency.

[4] Unpublished Flat Plate Rocket Exhaust Impingement Data Obtained for a 20:1 Scale F-1 Rocket Engine from Marshall Space Flight Center, Huntsville, Ala.

[5] Abramovich, G. M., "Theory of Turbulent Jets," AD 283-858, 1962, Armed Services Technical Information Agency.

[6] Johannesen, N. H., "Further Results on the Mixing of Free Axially Symmetrical Jet of Mach Numbers 1.40," ARC-20, 981, ASTIA AD 228 024, 1959, Aeronautical Research Council.

[7] Pitkin, E. T. and Glassman, I., "Experimental Mixing Profiles of a Mach 2.6 Free Jet," *Journal of the Aerospace Sciences*, Vol. 25, No. 12, Dec. 1958, p. 791.

[8] South, J. F., Goodhart, R. F., and Dodson, T. L., "Pressure Temperature, and Noise Measurements in the Subsonic Region of the Terrier Guided Missile Booster, MK 12 MOD 0 (X-240) Exhaust Stream," Rept. 1712, July 1960, U.S. Naval Weapons Lab., Dahlgren, Va.

[9] Frauenberger, H. J. and Forbister, J. G., "The Axial Decay and Radial Spread of a Supersonic Jet Exhausting into Air at Rest," Rept. R.P.D. 34, ASTIA AD 89904, Dec. 1955, Royal Aircraft Establishment, Farnborough, England.

[10] Donaldson, C. duP. and Grey, K. E., "Theoretical and Ex-

perimental Investigation of the Compressible Free Mixing of Two Dissimilar Gases," *AIAA Journal*, Vol. 4, No. 11, Nov. 1966, pp. 2017–2025.

[11] Shirie, J. W. and Seubold, J. G., "Length of the Supersonic Core in High Speed Jets," *AIAA Journal*, Vol. 5, No. 11, Nov. 1967, pp. 2062–2064.

[12] Eggers, J. M., "Velocity Profiles and Eddy Viscosity Distributions Downstream of a Mach 2.22 Nozzle Exhausting to Quiescant Air," TN D-3601, Sept. 1966, NASA.

[13] "Studies Pertaining to Bambi Ballistic Missiles–Plume Wind-Tunnel Research Program," ZR-AP-061-24, April 1962, General Dynamics Astronautics, San Diego, Calif.

[14] "Summary Report Rocket Exhaust Impingement Study," TR E 1-67, Nov. 1968, FMC Corp., Northern Ordnance Div., Minneapolis, Minn.

[15] Van Driest, E. R., "The Problem with Aerodynamic Heating," *Aeronautical Engineering Review*, Oct. 1956, pp. 26–41.

[16] Jepps, G. and Robinson, M. L., "Convective Heating at the Deflecting Surface of a Rocket Launch-Pad," *Journal of the Royal Aeronautical Society*, July 1967, pp. 469–475.

[17] Fay, J. A. and Riddell, F. R., "Theory of Stagnation Point Heat Transfer in Disassociated Air," *Journal of Aerospace of the Sciences*, Vol. 25, No. 2, Feb. 1958, pp. 73–85.

[18] Thring, M. W. et al., *Combustion and Propulsion*, Pergamon Press, New York, 1958.

[19] Brown, B. and McArty, K. P., "Particle Size of Condensed Oxides from Combustion of Metalized Solid Propellants," *Eighth Symposium (International) on Combustion*, Williams and Wilkins, Baltimore, Md., 1962, p. 817.

APRIL 1970 J. SPACECRAFT VOL. 7, NO. 4

A Theory for Base Pressures on Multinozzle Rocket Configurations

J. P. Lamb,* K. A. Abbud,† and C. S. Lenzo‡
The University of Texas at Austin, Austin, Texas

A new analysis is given for turbulent base flowfields in multi-nozzle configurations. The specific case of adiabatic flow in a four-nozzle symmetrical ring cluster is considered. Inviscid plume boundaries are described approximately with circular arcs. Because of symmetry, viscous effects at the common plume confluence can be treated by a planar analysis and flow conditions at the origin of the reverse jet thereby determined. The reverse jet development is analyzed with an integral method, using an effective eddy viscosity which is related to that in the free shear layers at the plume boundaries. The base pressure distribution is determined from the reverse jet impingement on the base plane. Depending upon the nozzle height, both weak and strong interactions may occur. Results of the present analysis are in general agreement with cold flow test data for a wide range of geometric variables.

Nomenclature

b_r = radius of reverse jet at cutoff station
C = Crocco number, $u(2c_pT_0)^{-1/2}$
E_1 = $\int_0^1 \tilde{\varphi}(1 - C_r^2\tilde{\varphi}^2)^{-1}\, d(y/b_r)$
E_2 = $\int_0^1 \tilde{\varphi}^2(1 - C_r^2\tilde{\varphi}^2)^{-1}\, d(y/b_r)$
F_1 = $4(\ln 2)^2C_c^2(1 - C_c^2)/F_2$
F_2 = $r_m(1 - 0.25C_c^2)[1 + (2\ln F_3 + C_c \ln F_4)]/\ln(1 - C_c^2)$
F_3 = $(1 - 0.25C_c^2)/(1 - C_c^2)$
F_4 = $(1 + 0.5C_c)(1 - C_c)/(1 - 0.5C_c)(1 + C_c)$
h = height of nozzle exit above base plane
H = $(S/2)$ sec 45°, see Fig. 4
I_1 = $\int_{-\infty}^{\eta} \varphi(1 - C_2^2\varphi^2)^{-1}d\eta$
I_2 = $\int_{-\infty}^{\eta} \varphi^2(1 - C_2^2\varphi^2)^{-1}d\eta$
k = c_p/c_v
L = length of plume boundary, see Fig. 1
M = mach number
$\dot{M}$ = momentum flow rate, $\int \rho u^2 dA$
m = mass flow rate, $\int \rho u\, dA$
P_b = static pressure at edge of base = ambient pressure
P_{0B} = base plane pressure at vehicle center
P_p = base plane pressure distribution
R_n = radius of nozzle exit
R_{pm} = maximum radius of inviscid plume boundary, see Fig. 1
r = radius of reverse jet
S = center-to-center spacing of nozzles on base plane, see Fig. 6
u = longitudinal velocity
Y = transverse coordinate in free layer
Z = axial coordinate along vehicle centerline
Z_{pm} = axial location of R_{pm}, see Fig. 1
β, δ, γ = angles, see Fig. 3
ϵ = nozzle expansion ratio
η = $\sigma y/L$
θ = angle measured from nozzle wall, Fig. 1
σ = spread rate parameter for free layer
ϕ = reverse jet velocity, $\tilde{u}/\tilde{u}_c = \exp[-(\ln 2)(r/r_m)^2]$
φ = free layer velocity, u/u_2
ψ = angle of plume boundary, see Fig. 1
ω = angle of meridian plane, see Fig. 2

Subscripts

0 = stagnation conditions
2 = freestream at edge of inviscid plume
amb = ambient
c = reverse jet centerline, see Fig. 5
d = dividing streamline of free layer
e = end of nonisobaric jet, see Fig. 5
i = nozzle exit
j = jet boundary streamline of free layer
m = average velocity in reverse jet

Presented as Paper 69-570 at the AIAA 5th Propulsion Joint Specialist Conference, U.S. Air Force Academy, Colo., June 9–13, 1969; submitted May 21, 1969; revision received January 27, 1970. This research was partially sponsored by NASA under Contract NAS 8-20321 with Marshall Space Flight Center.

* Associate Professor of Mechanical Engineering. Member AIAA.
† Research Engineer.
‡ Research Engineer. Member AIAA.